Ultrasonics Sonochemistry 19 (2012) 1039–1043

Contents lists available at SciVerse ScienceDirect

Ultrasonics Sonochemistry

journal homepage: www.elsevier.com/locate/ultsonch

Sonoelectrochemical synthesis and assembly of bismuth–antimony alloy: From nanocrystals to nanoflakes

Jian-Jun Shi [a,b], Yi-Jun Wang [a], Yue Ma [a], Qing-Ming Shen [a], Jun-Jie Zhu [a,*]

[a] State Key Laboratory of Analytical Chemistry for Life Science, School of Chemistry and Chemical Engineering, Nanjing University, Nanjing 210093, China
[b] School of Chemical Engineering, Anhui University of Science and Technology, Huainan 232001, China

ARTICLE INFO

Article history:
Received 21 January 2012
Received in revised form 17 February 2012
Accepted 2 March 2012
Available online 12 March 2012

Keywords:
Bismuth–antimony alloy
Sonoelectrochemistry
Nanoflakes
Crystals
Assembly
Synthesis

ABSTRACT

Bismuth-based nanostructures have attracted growing interest because of their promising thermoelectric properties and applications in optics and electronics. Pulsed sonoelectrochemical technique was selected to fabricate bismuth–antimony (BiSb) flake-like alloy in ethylene glycol aqueous solution. The formation mechanism for the BiSb alloy was discussed. Ultrasonic played an important role in regenerating electrode and promoting the formation of BiSb nanoflakes. Citrate and polyvinylpyrrolidone (PVP) were introduced as mixed controlling agents during the nucleation and growth process.

1. Introduction

Recently, semiconductor nanocrystals (NCs) and their clustered states in lower dimension present remarkable optical and electronic properties [1,2]. Synthesis and assembly of the nanoscale building blocks have been extensively studied [3–5]. Among these, Bi-based nanostructure has attracted growing interest because of its promising thermoelectric properties [6] and potential applications in optics and electronics [7], which was extensively employed to study the low-dimensional nanostructural properties related to quantum confinement effects, and self-assembly process [8]. Bi-rich alloys ($Bi_{100-x}Sb_x$, $x = 4–22$) exhibited semiconducting properties with the band gap of the order of 20–40 MeV [9]. However, it may be difficult to prepare homogeneous BiSb alloy nanoparticles via conventional techniques such as mechanical alloying [10], because the liquidus and solidus lines are apart from each other in the phase diagram of Bi–Sb system [11]. Electrochemical deposition has been proved to be an effective route for the fabrication of homogeneous Bi-based low-dimensional nanostructure [12], for instance, BiSb film and nanowire arrays [13–15]. It was also reported that chine-like BiSb alloy could be fabricated by a template-free electrodeposition method [16]. Ultrasound has showed the significant influence on the electrodeposition [17–19], especially on the synthesis of nanomaterials based on the effects of dispersion and cavitation [20,21]. Sonoelectrochemistry, which combines electrochemistry and ultrasonic technique [22], has been proven to be a fast, simple and effective route for the synthesis of nanoparticles [23–25]. However, to the best of our knowledge, there are no reports on the fabrication of BiSb alloy nanoflakes by this method.

Herein, sonoelectrochemical technique was used to synthesize and assemble BiSb nanoflakes. Citrate and polyvinylpyrrolidone (PVP) as mixed controlling agents were introduced in the formation of the BiSb nanoflakes. The morphology and structure of the product were characterized by TEM, EDS and XRD. A possible mechanism was also discussed.

2. Experimental

2.1. Materials

All chemical reagents were of analytical grade and used as received. PVP (K-30, Mw 40,000 Da) was purchased from Sigma–Aldrich, Co. Five hydration bismuth nitrates ($Bi(NO)_3{\cdot}5H_2O$), antimony tartrate potassium ($K(SbO)C_4H_4O_6{\cdot}1/2H_2O$), ethylene glycol, and tri-ammonium citrate ($(NH_4)_3C_6H_5O_7$) were purchased from Shanghai Chemical Reagent, Co. All solutions were prepared with deionized water from a water purification system (Millipore, Synergy). For pH adjustment, 0.1 M HCl and 0.1 M NaOH solutions were used.

2.2. Apparatus

A sonoelectrochemical device described previously [23,24] was employed to synthesize BiSb alloy without using a reference

* Corresponding author. Tel./fax: +86 25 83597204.
E-mail address: jjzhu@nju.edu.cn (J.-J. Zhu).

1350-4177/$ - see front matter © 2012 Elsevier B.V. All rights reserved.
http://dx.doi.org/10.1016/j.ultsonch.2012.03.001

electrode. A titanium horn (VC-750, Sonics & Materials) was used as both the cathode and the ultrasound emitter with an effective area of 1.23 cm^2 at the bottom. A platinum sheet (1.0 × 1.0 cm) was used as counter electrode. The ultrasonic system worked at an emission frequency of 20 kHz. The characterization of the ultrasonic power output was performed using a standard calorimetric method [26]. Unless otherwise indicated, the wave amplitude was adjusted to 30% of the maximum value.

2.3. Preparation of BiSb alloy nanosheet

In a typical synthesis, 0.012 M $Bi(NO_3)_3$, 0.002 M $(NH_4)_3C_6H_5O_7$, 0.012 M $K(SbO)C_4H_4O_6$, and 3.0 g L^{-1} PVP were dissolved into 60 ml of the mixture of ethylene glycol and water with a volume ratio of 1:1 under stirring.

The pH value of the mixture was then adjusted to 6.0. The solution was degassed with ultrapure N_2 prior to experiment. The electrochemical workstation (CHI6301B, USA) produced a current pulse (50 mA, 0.5 s) immediately following an ultrasonic pulse (25 W, 0.3 s) and 0.2 s of silence. Product was obtained after 3000 cycles of pulse-repetition, followed by centrifugation, washing and dispersion in ethylene glycol/water solution for several times.

2.4. Characterization

The morphology of the sample was characterized by high-resolution transmission electron microscopy (HRTEM, JEOL-2100) with a 200-kV accelerating voltage. The alloy composition was obtained by energy dispersive X-ray spectroscopy (EDS, Shimadzu SSX-550). The X-ray diffraction (XRD) patterns were recorded on an X-ray diffractometer (Shimadzu XD-3A) with a Cu–K X-ray source (λ = 0.15418 nm). The voltammetric behavior in the preparation process was investigated by cyclic voltammetry (CV) and linear sweep voltammetry (LSV) using a CHI 660D electrochemical workstation (CH Instruments Co., USA) in a conventional three-electrode system, which comprised of a platinum sheet auxiliary electrode, titanium working electrode and a saturated calomel reference electrode.

3. Results and discussion

3.1. Characterization of BiSb alloy

As shown in Fig. 1A and B, flake-like BiSb alloy composed of small particles was prepared. The typical HRTEM image in Fig. 1B reveals that the *d*-spacing of adjacent fringes for the nanocrystals is 0.32 nm, corresponding to the (012) plane of primitive hexagonal BiSb alloy. In Fig. 1C, the presence of Bi and Sb in the nanoflakes was also confirmed by EDS, and the result of elemental analysis is shown in the inserted table. The atomic ratio of Bi and Sb are approximately 78% versus 22%, which is also in good agreement with the results from XRD patterns.

The XRD was used to characterize the structure of the BiSb alloy nanoflakes. In Fig. 2, all the diffraction patterns clearly show three main characteristic peaks, which can be indexed to a single-phase hexagonal rhomb-centered (*hrc*) structure (JCPDS No. 35-0517). The peaks of the BiSb alloy appear between that of pure Bi and Sb, which indicates that the alloy is obtained without phase separation. In addition, the average size of BiSb nanoparticles is ca. 10 nm from Debye–Scherrer equation, which is consistent with the HRTEM results.

3.2. Voltammetric study of the sonoelectrochemical process

Voltammetry was used to study the alloy electrodeposition. The reduction potential of different ratio of Bi(III) and Sb(III) was also investigated. As shown in Fig. 3A, the deposition potential of Sb(III) (−1.2 V, curve e) was more negative than that of Bi(III) (−0.9 V, curve a), indicating that Sb(III) was more difficult to be reduced than Bi(III). The separated reduction peaks were also observed for the mixed solution of Bi(III) and Sb(III) without PVP as shown in Fig. 3A, inset. However, for each of the mixed electrolyte containing PVP, only one reduction peak between −0.8 and −1.0 V was observed in Fig. 3A, b–d, indicating the co-deposition of Bi and Sb occurred [16,27], . LSV was performed with and without sonication (25 W, 0.3 s) to investigate the reproducibility of the repeated cycles that

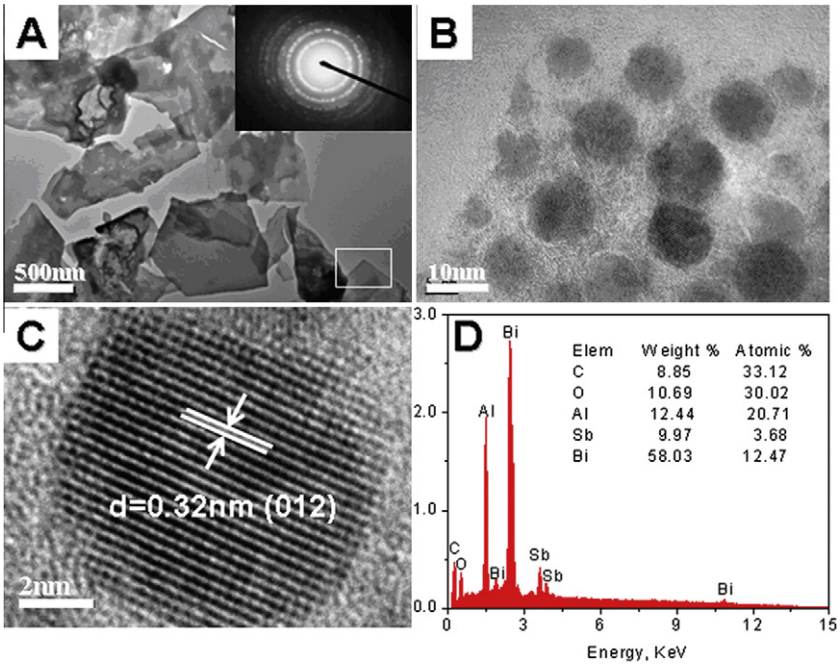

Fig. 1. Low-magnification TEM image (A) and SAED (inset of A), high-magnification TEM (B), the crystal structure (C), and the corresponding EDS spectrum (D) of the flake-like BiSb alloy,

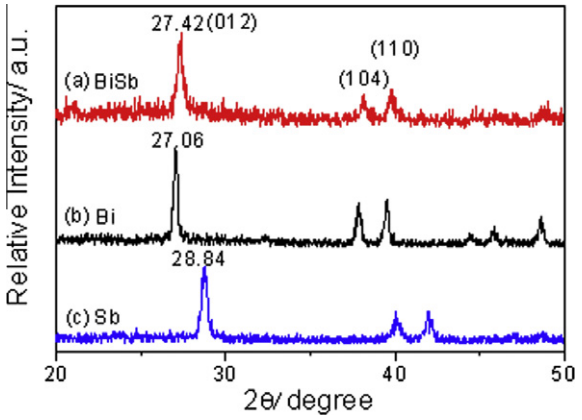

Fig. 2. the XRD patterns of the BiSb alloy (a), pure Bi (b), and Sb (c).

composed of alternating ultrasonic and electrodeposition pulses. In Fig. 3B, the co-deposition potential shifts negatively with the repeated scanning without sonication, and get back after an ultrasonic pulse, which suggests that the sonoelectrode was reproducible by removing of primary BiSb alloy particles and dispersing them into solution to leave a clean surface for the reaction to continue [28].

3.3. Formation mechanism of the BiSb alloy

The evolution for the synthesis and assembly of the BiSb nanoflakes was performed at different durations by TEM images observation. As shown in Fig. 4A, the primary BiSb NCs were obtained after 400 cycles of sonoelectrochemical reaction which was similar to the four-step evolution described in our previous report [29], involving the diffusion of the Bi(III) and Sb(III) complex ions, the co-deposition of the primary BiSb NCs, the vibration and dispersion from the electrode surface. Consequently, with the increasing amount of BiSb, net-like structure could be observed in ethylene glycol/water solution as shown in Fig. 4C, and eventually led to the formation of BiSb nanoflakes (Fig. 4D). In Fig. 4D, inset, the flakes grew larger because of the oriented attachment of the newly generated BiSb NCs at certain faces in the presence of PVP [30].

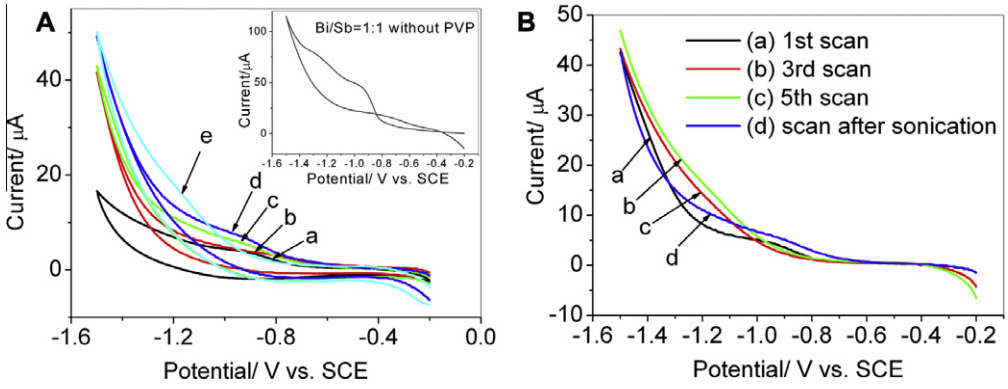

Fig. 3. (A) *CV* curves for pure Bi(III) (a), mixed solutions of Bi(III) and Sb(III) at molar ratio of 1:1 (b), 1:2 (c), 2:1 (d) and pure Sb(III) (e) in the presence of PVP, the inset was the CV for Bi/Sb = 1:1 without PVP; (B) LSV curves obtained at Ti sonoelectrode with ((a) first scan, (b) third scan, (c) fifth scan) or without (d) an ultrasonic pulse followed, where scan range was −0.2 to −1.5 V vs. SCE, scan rate was 50 mV s^{-1}, under N_2-saturated atmosphere.

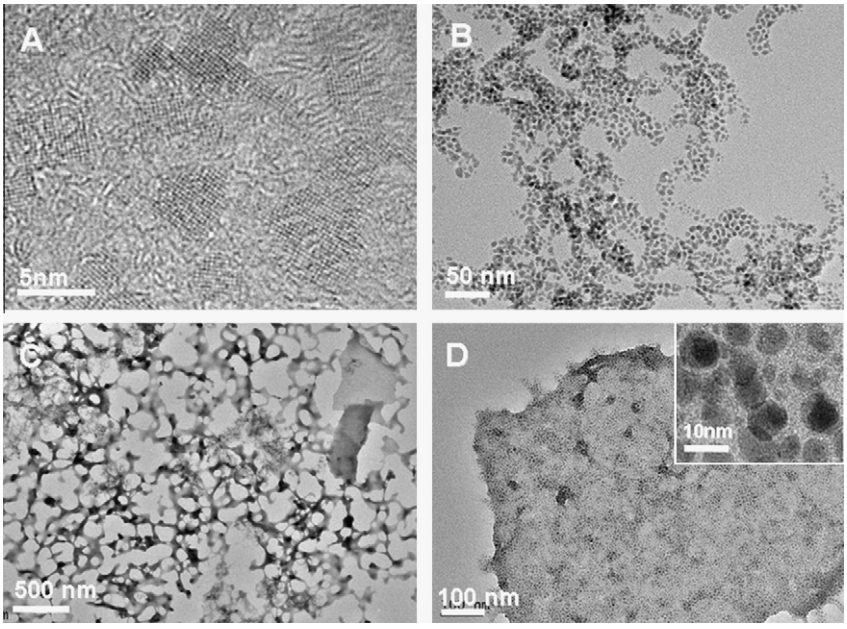

Fig. 4. TEM images of the BiSb alloy prepared via sonoelectrochemistry after different reaction times of 400 s (A), 600 s (B), 1000 s (C) and 1600 s (D). Corresponding HRTEM are shown in the inset images.

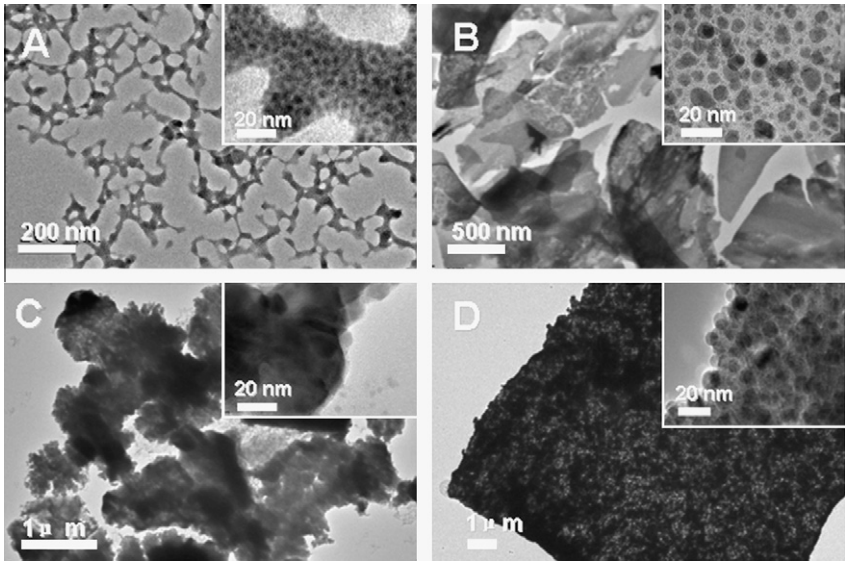

Fig. 5. TEM images of the BiSb alloy prepared by adding PVP with the amount of 0.5 g (A), 0.2 g (B), 0.05 g (C) and none (D). Corresponding HRTEM are shown in the inset images.

Eventually, well-dispersed BiSb nanoflakes were obtained by repeating above procedures as observed in Fig. 1A.

3.4. Influence of synthetic conditions on the fabrication of BiSb nanoflakes

Both the sonication and the additives are essential for the fabrication of the flake-like structures of BiSb alloy. The sonoelectrochemical processes were influenced by the different physical mechanisms such as acoustic streaming, microstreaming and turbulence due to cavitation, and formation of microjets in the course of collapse of cavitation bubbles [20–24]. The convection caused by microturbulence and shock waves was an important factor affecting nucleation and growth rate [31]. Ultrasonic also played a crucial role in regenerating electrode and promoting the formation of BiSb nanoflakes. While the additives, involving citrate, ethylene glycol and PVP, were necessary in the present synthesis for the fabrication of BiSb alloy nanoflakes. Namely, citrate anions played an important role in the formation of the spherical BiSb NCs due to the nonselective adsorption. Meanwhile, ethylene glycol acted as both the solvent and the stable agent by the formation of a protective layer via an interaction between its OH group and the surface of obtained particles [32]. Additionally, PVP showed a predominantly adsorption on the (0 1 2) planes of the BiSb NCs, which originate from the lone pair of oxygen atoms in carboxides and nitrogen atoms in pyrrolidone rings [33], leading to the formation of nanoflakes by oriented assembly. PVP may act as some face-inhibited function surfactant during the anisotropic growth of BiSb nanoflakes, which determines the subsequent shape of the crystals.

The influence of the amount of PVP was further studied. As shown in Fig. 5, the variation of the PVP concentration could lead to the formation of different morphologies. Compared with typical image of BiSb nanoflakes in Fig. 5B, an excessive amount of PVP prevented the formation of 2D plane, due to the spatially separation caused by PVP film wrapping around each particle [34] as shown in Fig. 5A. While the PVP concentration decreased to 0.75 g L^{-1}, the agglomerates composed of irregular particles were observed in Fig. 5C. Fig. 5D showed the compact structure obtained in the absence of PVP, whereas, the formation of spherical BiSb NCs can also be attributed to the nonselective adsorption of citrate in the ethylene glycol/water medium.

4. Conclusion

In summary, flake-like BiSb alloy nanostructure was synthesized by a sonoelectrochemical method in ethylene glycol/water solution. A possible formation mechanism was suggested as coupled synthesis and assembly of BiSb nanocrystals to nanoflakes. Citrate and PVP acted as mixed controlling agents during the nucleation and growth process. Meanwhile, ultrasonic played a crucial role in regenerating electrode and promoting the formation of BiSb nanoflakes. This method is also expected to prepare other Bi-based nanomaterials with 2D structures, which have promising thermoelectric properties and potential applications in optics and electronics.

Acknowledgements

We greatly appreciate the support of the National Natural Science Foundation of China (Nos. 21071004 and 21121091) and National Basic Research Program of China (2011CB933502). We also thank the support of International S&T Cooperation Projects of China (2010DFA42060). J.-J. Shi also thanks the support of Anhui Provincial Natural Science Foundation (1208085MB27).

References

[1] A.P. Alivisatos, Semiconductor clusters, Science 271 (1996) 933.
[2] D.V. Talapin, J.S. Lee, M.V. Kovalenko, E.V. Shevchenko, Chem. Rev. 110 (2010) 389.
[3] X.G. Peng, Chem. Eur. J. 8 (2002) 335.
[4] Z.Y. Tang, Z.L. Zhang, Y. Wang, S.C. Glotzer, N.A. Kotov, Science 314 (2006) 274.
[5] R.K. Mallavajula, L.A. Archer, Angew. Chem. Int. Ed. 50 (2011) 578.
[6] N. Ando, T. Kiyabu, H. Kitagawa, M. Itoh, Y. Noda, Physica B 329 (2003) 1540.
[7] G. Bihlmayer, Y.M. Koroteev, E.V. Chulkov, S. Blügel, New J. Phys. 12 (2010) 065006.
[8] L. Li, X.C. Dou, H.Q. Wang, G.H. Li, L.D. Zhang, Pure Appl. Chem. 82 (2010) 2075.
[9] B. Lenoir et al., J. Phys. Chem. Solids 57 (1996) 89.
[10] Soma Dutta, V. Shubha, T.G. Ramesh, Florita D'Sa, J. Alloys Compd. 467 (2009) 305.
[11] B. Lenoir, A. Demouge, D. Perrin, H. Scherrer, S. Scherrer, M. Cassart, J.P. Michenaud, J. Phys. Chem. Solids 56 (1995) 99.
[12] F. Xiao, C. Hangarter, B. Yoo, Y. Rheem, K.H. Lee, N.V. Myung, Electrochim. Acta 53 (2008) 8103.
[13] M.M. González, A.L. Prieto, M.S. Knox, R. Gronsky, T. Sands, A.M. Stacy, Chem. Mater. 15 (2003) 1676.
[14] X.C. Dou, G.H. Li, X.H. Huang, L. Li, J. Phys. Chem. C 112 (2008) 8167.
[15] X.C. Dou, G.H. Li, H.C. Lei, Nano Lett. 8 (2008) 1286.

[16] B. Zhou, X.H. Li, J.J. Zhu, Cryst. Growth Des. 7 (2007) 2276.
[17] V. Sáez, J. Gonzalez-García, J. Iniesta, A. Frías-Ferrer, A. Aldaz, Electrochem. Commun. 6 (2004) 757.
[18] B.G. Pollet, Electrochem. Commun. 11 (2009) 1445.
[19] R.G. Compton, C.E. Banks, Understanding Voltammetry, second ed., World Scientific, Singapore, 2010.
[20] A. Gedanken, Ultrason. Sonochem. 11 (2004) 47.
[21] J.H. Bang, K.S. Suslick, Adv. Mater. 22 (2010) 1039.
[22] V. Sáez, T.J. Mason, Molecules 14 (2009) 4284.
[23] Q.M. Shen, Q.H. Min, J.J. Shi, L.P. Jiang, W.H. Hou, J.J. Zhu, Ultrason. Sonochem. 18 (2011) 231.
[24] J.J. Shi, G.H. Yang, J.J. Zhu, J. Mater. Chem. 21 (2011) 7343.
[25] Y. Zhao, H. Pan, Y. Lou, X. Qiu, J.J. Zhu, C. Burda, J. Am. Chem. Soc. 131 (2009) 4253.
[26] M.A. Margulis, I.M. Margulis, Ultrason. Sonochem. 10 (2003) 343.
[27] A.J. Bard, L.R. Faulkner, Electrochemical Methods, Fundamentals and Applications, second ed., John Wiley and Sons, Inc., Hoboken, NJ, 2001.
[28] M.E. Hyde, R.G. Compton, J. Electroanal. Chem. 531 (2002) 19.
[29] J.J. Shi, J.J. Zhu, Electrochim. Acta 56 (2011) 6008.
[30] W.Z. Wang, B. Poudel, Y. Ma, Z.F. Ren, J. Phys. Chem. B 110 (2006) 25702.
[31] V.S. Nalajala, V.S. Moholkar, Ultrason. Sonochem. 18 (2011) 345.
[32] A. Datta, J. Paul, A. Kar, A. Patra, Z.L. Sun, L.D. Chen, J. Martin, G.S. Nolas, Cryst. Growth Des. 10 (2010) 3987.
[33] Y.G. Sun, Y.N. Xia, Science 298 (2002) 2176.
[34] B.A. Rozenberga, R. Tenneb, Prog. Polym. Sci. 33 (2008) 40.